

# UPGRADE OF THE 25 MW RF STATION FOR THE LINEAR ACCELERATOR LINAC2 AT ELSA

D. Proft\*, K. Desch, D. Elsner, M. Switka, Physics Institute, University of Bonn, Germany

## Abstract

At the Electron Stretcher Facility ELSA in Bonn the first acceleration stage consists of a 3 GHz traveling wave linear accelerator. It was powered by a 25 MW pulsed high power klystron amplifier, which had been in use for the last thirty years. After a major failure and due to the lack of spare part availability the RF station was rebuilt. In addition to a new klystron including its high voltage tank, the new setup also consists of major upgrades of the infrastructure, the pulse forming network and the safety interlocks to satisfy the contemporary requirements.

A new monitoring system consisting of multi-channel sampling ADCs allows for automatic pulse-by-pulse analysis of the klystron parameters and simultaneous evaluation of RF performance and stability.

In this contribution we will present the new RF station setup, which has successfully been operating since the beginning of 2021 as well as the new monitoring capabilities.

## ELECTRON STRETCHER FACILITY

At the Electron Stretcher Facility ELSA (see Fig. 1) polarized or unpolarized electrons are accelerated to energies of up to 3.2 GeV within a three-staged accelerator scheme including a Linac, the Booster Synchrotron and the ELSA stretcher ring [1]. The first and second stage of the facility are synchronized to the mains frequency of 50 Hz and consist of either a source for polarized electrons or a thermionic gun, operated at 50 kV and a traveling wave Linac. The following Booster Synchrotron further accelerates the electrons and transfers them to the main storage ring at an energy of 1.2 GeV. After accumulating typically 30 mA in the stretcher ring, the electrons are accelerated to 3.2 GeV and then slowly extracted to either two experimental sites for hadron physics experiments (E1 and E2) or to a second beamline dedicated for detector testing (E3) at user controllable rates between 200 Hz and 625 MHz.

### Linac Section

The S band Linac (LINAC2) is used to accelerate 1  $\mu$ s long electron pulses with a charge of up to 100 nC to a central energy of 26 MeV with an energy spread of below 5%. It is powered by a 12.5 MW RF station with a frequency of 2.9987 GHz.

As the transfer beamline to the booster synchrotron comprises a 90° deflection dipole (see Fig. 1, lower left), a slit system behind the magnet is used in the feedback loop of a PID controller to stabilize the central electron energy by slightly adjusting the RF power provided to the Linac.

\* proft@physik.uni-bonn.de

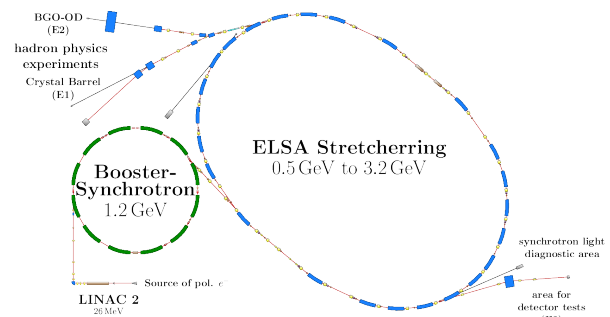


Figure 1: Sketch of the electron stretcher facility ELSA.

## RF STATION UPGRADE

As the previously installed Linac klystron<sup>1</sup> showed degraded performance, major parts of the RF station were reconstructed in favor for a new type of klystron<sup>2</sup>. With the klystron a new high voltage tank, including a new pulse transformer, was installed.

Furthermore, major parts of the infrastructure (e.g. cooling system and its monitoring, SF6 gas handling in the waveguides, auxiliary power supplies with digital PLC interface) were also upgraded and extended to match the requirements. A new thyristor-based power supply for heating of the klystron's filament was developed in-house. It allows for stabilization of the heater current within 0.5% and long term drifts smaller than 0.75% at a peak output power of 1 kW.

Table 1: Modulator Specifications

Property	Value
PFN total capacity	650 nF
PFN impedance	4.3 $\Omega$
peak (nominal) PFN voltage	30 kV (26.5 kV)
HV pulse duration	ca. 4 $\mu$ s
RF pulse duration	ca. 3 $\mu$ s

The existing modulator (for specs see Table 1), consisting of a high voltage power supply (HVPS) for charging of the pulse forming network's (PFN) capacitors to 30 kV, was largely reused with the new setup. The PFN's impedance and HV pulse duration were compatible. Nevertheless, a new tail clipper diode assembly for suppression of reflections from the klystron tank was installed into the PFN cabinet as replacement to the previously installed one that was located inside the tank but had to be disassembled due to space constraints.

<sup>1</sup> F2042E by Thomson-CSF, France

<sup>2</sup> TH2100D by Thales, France

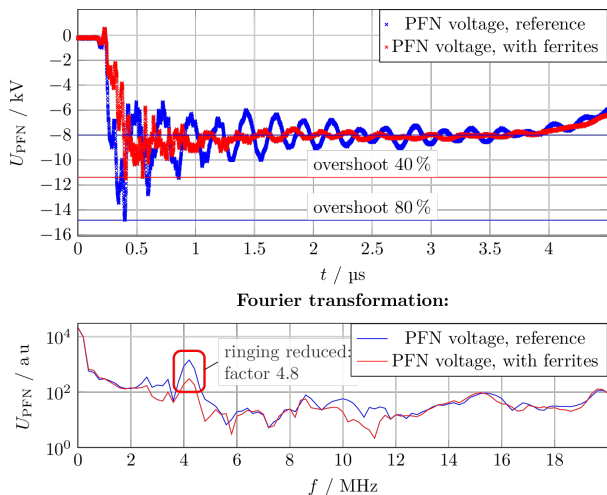


Figure 2: PFN voltage pulse  $U_{\text{PFN}}$  and corresponding Fourier transformation measured at the HV cable terminal without (blue) and with (red) ferrites installed at  $U_{\text{HVPS}}$  of 15 kV.

The existing stand-alone 3 GHz-signal generator with subsequent pre-amplifying klystron with an output power of up to 180 W with 3  $\mu\text{s}$  pulse duration could be reused. Due to the much higher amplification gain of the new klystron in respect to the old one the required power is now limited to below 13 W.

### Ringings & Ferrite Reactor

During the first commissioning stage a large ringing with a frequency of  $f_{\text{ring}} = 4.3 \text{ MHz}$  and overshoot of 80 % was observed on the PFN output voltage  $U_{\text{PFN}}$  (see Fig. 2, blue and Fig. 3). Countermeasures for these distortions have been implemented, as the large overshoot of almost twice the signal height introduces stress on the dielectric medium of the high voltage cable connecting the PFN to the klystron tank. The corresponding ringing had been also noticeable on the secondary side of the klystron tank's HV pulse transformer.

Simulations of an equivalent circuit with ngspice revealed, that stray capacitances  $C_s$  of the newly installed tail clipper diode and the HV cable together with the stray inductance  $L_s$  of the pulse transformer formed a resonant circuit that is excited by the steep voltage slope right after thyatron switch-on. This was confirmed by altering the stray capacitance by bypassing up to 13 of the 20 diodes connected in series for the tail clipper diode arrangement. With different values for the stray capacitance  $C_s + \Delta C$  the shift of the

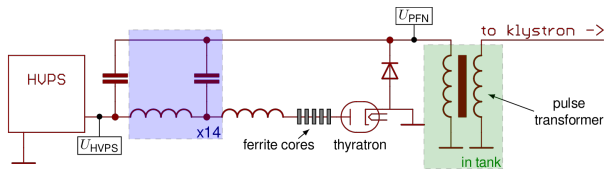


Figure 3: Minimized schematics of the PFN circuit showing the position of the newly installed ferrites.

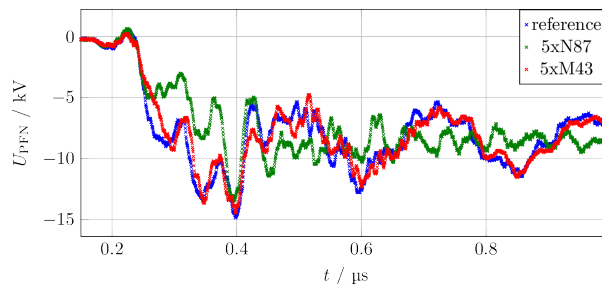


Figure 4: First part of the PFN voltage pulse  $U_{\text{PFN}}$  with different ferrites installed and without ferrites as reference (blue).

corresponding resonance frequency  $\omega (\Delta C)$  of the circuit given by

$$\omega (\Delta C) = \frac{1}{\sqrt{L_s \cdot (C_s + \Delta C)}} ,$$

can be measured via Fourier transformation of  $U_{\text{PFN}}$  (compare Fig. 2 for frequency spectrum with 20 connected diodes resulting in  $\Delta C = 0$ ). Finally,  $C_s = 2.76(33) \text{ nF}$  and  $L_s = 503(52) \text{ nH}$  could be determined.

As a countermeasure the installation of an RC snubber circuit on the PFN output was considered, but was discarded due to severe reduction of the usable HV pulse flattop duration and thus limiting the utilizable RF pulse duration. Furthermore the installation of a low inductance high voltage resistor beside a high voltage capacitance inside the PFN cabinet would have required a complete reconstruction of the cabinet.

A more compact approach was given by the installation of ferrite ring cores around the terminal of the thyatron to introduce a lossy absorber and thus reduce the ringing as well as the overshoot [2]. A wide variety of ferrites with base materials  $MnZn$  and  $NiZn$  and different compositions was tested, that were selected based on the permeability  $\mu$ , the magnetic flux density at saturation  $B_{\text{max}}$ , the coercivity  $H_c$  and the remanence  $B_r$ . Additionally, materials with peak amplitude of the complex permeability  $\mu''_s$  in the range of  $f_{\text{ring}}$  were chosen. As the thyatron terminal connection has a diameter of 35 mm, the geometric properties were chosen depending on the inner diameter and a sufficiently large surface area.

As an example, in Fig. 4 the first 0.8  $\mu\text{s}$ -portion of the PFN voltage pulse  $U_{\text{PFN}}$  for a selection of two materials (*N87* and *Material 43*, compare Table 2) at half of the maximum HVPS voltage (15 kV) is shown. Similar measurements were conducted for each material with multiple different quantities of ferrites. Based on these findings, a combination of different materials and geometric dimensions was installed, that was verified to be the best choice with respect to a suppression of the overshoot and reduction of the ringing during the pulse's flat top. The final composition consists of 4x*N87*, 2x*Material 43* and 6x*3C90* ferrites and is depicted in Fig. 5. It yields a decreased ringing by a factor of 4.8 and a suppression of the overshoot by a factor of two. Moreover, with

Table 2: Specifications for Different Ferrites

Material	3C90	N87	Mat. 43
manufacturer	Ferroxcube	TDK	Fair Rite
base material	MnZn	MnZn	NiZn
$\mu$	2300	2200	800
$B_{\max}$ / mT	470	490	350
$H_c$ / A m <sup>-1</sup>	16	21	29
$B_r$ / mT	170	175	220
Peak $\mu_s''$ / MHz	2	1.1	4
inner diameter / mm	37.7/39.7	36	35.6
outer diameter / mm	63.4/80.4	65.3	61
width / mm	25.3/15.3	26.6	12.7



Figure 5: Ferrite cores (2xN87, 1xMat. 43, 6x3C90, 1xMat. 43, 2xN87) consisting of three different materials and sizes.

the use of the ferrites the utilizable flat top pulse duration is decreased only by less than 100 ns. The corresponding pulse and Fourier transformation are shown in Fig. 2 (red).

Furthermore it was evaluated that an inverse pre-magnetization (and thus an increased hysteresis loss) of the ferrites can increase the overall suppression. Therefore, the HVPS was connected directly to the thyatron terminal leading to the HVPS current flowing in opposite direction through the ferrites during loading of the capacitors. As the maximum HVPS charging current is limited to 1 A, no noteworthy effect could be monitored.

### New Waveguide

The existing vacuum window<sup>3</sup>, a waveguide section including a 50 dB directional coupler and a hybrid splitter adjacent to it for powering a 3 GHz prebuncher remained in use to avoid breaking of the Linac structure's vacuum. As the waveguide dimensions of 66.4 mm × 29.5 mm differ from the WR284 waveguide output of the new klystron an interconnecting taper adapter was required. Due to long manufacturer lead times, a short taper with length  $l_{\text{taper}} = 26.25$  mm was made of stainless steel in the university machine shop instead of one with the ideal length [3] of  $l_{\text{taper}} = 72.33$  mm. Simulations with CST<sup>4</sup> predict a resulting VSWR = 1.04 which is considered acceptable, but could be improved in the future (VSWR = 1.002 for an ideal taper length). Directly before the taper an additional 50 dB directional coupler is mounted. With this the waveguide could be verified to operate sufficiently with a klystron output power of  $P_{\text{out}} \approx 15$  MW at a VSWR of 1.30(3) including the reflections at the Linac structure.

<sup>3</sup> TH19417 by Thomson-CSF, France

<sup>4</sup> CST Studio Suite, *CST Microwave Studio*, 2008. <http://www.cst.com>

## MONITORING

The safety interlock and monitoring system based on a PLC was completely revised to support the new power supplies connected via PROFIBUS. The interlock's response time is lower than 8 ms, thus being capable of shutting down the modulator after one faulty pulse or in case of violated operation conditions.

### Pulse Monitoring

A real-time pulse monitoring system is currently under commissioning that is capable of digitizing the PFN voltage pulses, the klystron current and voltage pulses as well as the forward and reflected RF pulse amplitudes measured by directional couplers in the waveguide. The monitoring system uses an in-house developed 32 channel differential FPGA-based sampling ADC [4] with 40 MSPS per channel. The input pulse shaper and amplification of each channel were adjusted individually to enable for full 16 bit resolution in the digitization chain. The FPGA sends the digitized pulses (512 data points per channel) via Ethernet to a computer from where they are distributed for further processing. Hence the system is able to analyze the signals provided on a pulse-by-pulse basis. From each pulse several features, such as flattop amplitude (and RMS), rise time and integral are extracted and either brought to display in the control system or used as (slow) interlock criterion for machine protection. In case of detection of erroneous pulse shapes a shutdown within 100 ms (worst case) is achievable. In this way, it enables for early detection of degradation effects regarding the klystron output power as well as online performance monitoring.

## SUMMARY & OUTLOOK

The new modulator and klystron have been successfully operating since the beginning of 2021 with excellent reliability and  $\approx 3000$  operation hours. The ongoing improvements include the finalization of the pulse-by-pulse monitoring and its integration into the interlock and control system.

As a future upgrade, the replacement of the existing 3 GHz generator and the pre-amplifying low power klystron by a solid state amplifier is currently evaluated. Furthermore, it is currently examined if a low level RF system can be installed for beam loading compensation, and thus, reduction of the energy spread of the Linac.

## REFERENCES

- [1] W. Hillert, "The Bonn Electron Stretcher Accelerator ELSA: Past and future.", *Eur. Phys. J. A* 28, pp. 139–148, 2006. doi: 10.1140/epja/i2006-09-015-4
- [2] A. R. Donaldson, "A Hybrid Anode Reactor for the SLAC Modulator", *21th Int'l Power Modulator Symposium*, 1994
- [3] A. F. Harvey, "Microwave Engineering", Academic Press, London, 1963
- [4] J. S. Müllers, "An FPGA-based Sampling ADC for the Crystal Barrel Calorimeter", 2019. <https://nbn-resolving.org/urn:nbn:de:hbz:5n-56693>